June 2023

Phase Transitions in the Two-Higgs-Doublet Model with a Softly-Broken $\mathbb{Z}_2$ Symmetry

Filip Gustavsson

Department of Physics, Lund University

Bachelor thesis supervised by Johan Rathsman

LUND
UNIVERSITY

Abstract

The two-Higgs-doublet model (2HDM) is an extension to the Standard Model which adds a second Higgs doublet. This extension provides freedom within the model, in comparison to the Standard Model, which makes it possible to study strong electroweak phase transitions. These can provide an explanation for the matter-antimatter asymmetry through the Sakharov conditions, three conditions that leads to creating this asymmetry in the early universe. Due to this, we are looking at phase transitions in the 2HDM extension to the Standard Model. This is done by using an effective field theory, dimensional reduction, that allows to study thermal effects in the model. Using this, a search is done which finds strong phase transitions for certain parameters. These results are compared to another method that has been previously used without finding a good similarity between the results for the different methods.

Populärvetenskaplig Beskrivning

Efter upptäckten av Higgspartikeln vid CERN 2012 har alla partiklar i standardmodellen för partikelfysik upptäckts. En intressant frågeställning är då för vilka processor inom fysiken som standardmodellen är bristfällig och inte ger tillfredsställande svar. Fysik som försöker utvidga partikelfysiken till mer än standardmodellen i hoppet om att kunna ge svar på dessa frågor kallas fysik bortom standardmodellen. Ett exempel på en sådan typ av fysik är försöket till en förklaring på varför allt kring oss är materia medan antimateria är så otroligt sällsynt att det tog fysiker till 1900-talet att upptäcka det. Det här projektet undersöker en utvidgning av standardmodellen och om den har egenskaper som möjliggör en förklaring på detta fenomen kring materia och antimateria.

Fysikern Andrei Sakharov ger en del av förklaringen till bristen på symmetri mellan materia och antimateria. Han lade fram tre krav som leder till processer i det tidiga universum som skapar denna asymmetri. Dessa krav är relaterade till partiklars egenskaper och flera av dem är inte möjliga att uppfylla inom standardmodellen. Detta motiverar att undersöka en utvidgning av standardmodellen för att möjliggöra den frihet, inom den utvidgade modellen, som behövs för att kunna möta dessa krav. Det krav som fokuseras på specifikt i detta projekt är att det tidiga universum inte ska vara i termisk jämvikt. Denna jämvikt råder i ett system när det inte sker någon transport av värme inom detta system vilket även gör att inga temperaturskillnader kan förekomma inom systemet.

Utvidgningen av standardmodellen som används i det här projektet är den så kallade tvåhiggsdubblet-modellen (2HDM) som, likt namnet antyder, har två Higgs dubbletter till skillnad från standardmodellen som enbart har en dubblett. Detta är av vikt eftersom den termiska jämvikten kan brytas av fasövergångar i Higgsmekanismen i det tidiga universumet. Dessa sker när universumet går från att ha en elektrosvag symmetri till att inte ha denna symmetri, symmetrin bryts. Detta symmetribrott är vad som ger massa till partiklar och kan även göra att det tidiga universum inte var i termisk jämvikt om fasövergången var stark. Styrkan på fasövergången beror på hur stor skillnad i energi det är från det

symmetriska tillståndet till den brutna symmetrin. I standardmodellen är förändringen inte stor nog för att bryta den termiska jämvikten medan i 2HDM är det möjligt för den att vara stor nog för att bryta den termiska jämvikten.

Det här projektet undersöker fasövergångar inom 2HDM och om de är starka eller ej. Undersökningen av fasövergångar sker genom en metod, dimensionell reducering, vilket jämförs med andra metoder för att finna dessa fasövergångar. Eftersom det är starka fasövergångar som är intressanta för frågan om materia och antimateria är det dessa fasövergångar som fokus läggs på. Projektet finner starka fasövergångar för en del parametrar i 2HDM och jämför dessa resultat med andra metoder för att studera fasövergångar.

Contents

1 Introduction

An unanswered question in the Standard Model (SM) is the cause of the matter-antimatter asymmetry that we observe today [1]. The process that would have created this asymmetry in the early universe is called baryogenesis, which could have been caused by the breaking of the electroweak symmetry [2]. This would have manifested as a type of phase transition (PT), more specifically an electroweak phase transition (EWPT). This PT occurred when the universe expanded and therefore cooled which resulted in a non-zero vacuum expectation value for the Higgs field [3].

While it is known that a PT can cause baryogenesis, the matter-antimatter asymmetry is still unexplained in the SM as all *Sakharov conditions* are not met. There are three conditions that must be met in order for the asymmetry to be explained by baryogenesis in the early universe. One of the conditions, that is not met in the SM, is the requirement that the early universe needs to not be in thermal equilibrium. This would be accomplished if the EWPT in the early universe was strong and first-order, which it is not in the SM but could be in extensions of it. Another condition is the presence of both C and CP violation in the early universe. While there is CP violation in the SM it is not strong enough to fulfill the requirement for the condition. The SM does however meet the final Sakharov condition, the violation of baryon number [2].

The Sakharov conditions provide motivation for a model with an additional Higgs doublet, the two Higgs-doublet model (2HDM), as in the 2HDM a strong first-order PT is possible [4]. The first introduction of the 2HDM, in Ref.[5], showed that this extension of the SM gives an additional source of CP violation. This means that all Sakharov conditions may be fulfilled in a 2HDM, which makes a model with baryogenesis possible in the 2HDM. This project will however only focus on the condition of having a strong EWPT.

In this paper the PT in the 2HDM will be investigated using a technique known as dimensional reduction [6]. This technique uses an effective theory that describes the temperature dependent properties of the theory well, given that the temperature is sufficiently high. The dimensional reduction is performed using DRalgo [7], a package developed for this purpose. While the PTs in the 2HDM have been looked at previously those searches tend to use other methods [8][9]. Therefore, it is of interest to examine how this method performs in comparison to other methods and in what way the results differs.

The paper goes through the procedure used to find PTs in the 2HDM as well as the background necessary regarding the 2HDM and PTs. In section 2 the general theory behind the 2HDM and PTs is presented. After that the specific parameters used to define the model are described in section 3 as well as how to convert between different sets of parameters. With this general information about the model, section 4 describes the techniques used to compute PTs. This section also explains DRalgo [7] and CosmoTransition [10], two packages which implement the algorithms necessary to calculate PTs. Using the numerical methods, section 5 goes through the different scenarios that were used in the search for PTs and what was found. It also analyzes the impact of internal parameters, i.e. order and matching scale, on the result of the model. Using these results, in section 6, conclusions are drawn about the results and methods used.

2 Background

The 2HDM adds an additional doublet to the Standard Model. In this section the background for it is introduced. Specifically, in section 2.1 the basics of the model in two different bases is presented and the notation is introduced. In addition to the theory of the model, the constraints needed to make the model unitary and stable are presented in subsection 2.2. Following that, section 2.3 introduces the basics of phase transitions in particle physics as well as concepts specific to phase transitions such as the strength and order of a phase transition. In section 2.4 the general method used for calculating PTs, as well as the justification behind it, is presented.

2.1 The Higgs Bases

This section contains general information about the 2HDM following the conventions in [11], a more comprehensive overview is available in [12]. In the generic basis the Higgs doublets in the 2HDM are written as

$$\Phi_1 = \begin{pmatrix} \phi_1^+ \\ (v_1 + \rho_1 + i\eta_1)/\sqrt{2} \end{pmatrix}, \Phi_2 = \begin{pmatrix} \phi_2^+ \\ (v_2 + \rho_2 + i\eta_2)/\sqrt{2} \end{pmatrix}. \tag{1}$$

From the 8 fields in the doublets, three of them are the would be *Goldstone bosons* [13]. These are in turn absorbed into the $W^\pm$ and Z bosons giving them mass. The other 5 fields combine to form five Higgs particles, meaning that the Φ_1 and Φ_2 doublets contain five Higgs particles.

In a CP-conserving theory these particles are the CP-even h and H, the CP-odd A and the charged $H^\pm$. The CP-even particles are differentiated by using a convention where

$$m_h \leq m_H, \tag{2}$$

and they are related to the ρ_1 and ρ_2 fields defined above by

$$\begin{pmatrix} H \\ h \end{pmatrix} = \begin{pmatrix} \cos(\alpha) & \sin(\alpha) \\ -\sin(\alpha) & \cos(\alpha) \end{pmatrix} \begin{pmatrix} \rho_1 \\ \rho_2 \end{pmatrix}, \tag{3}$$

where angle α is the *mixing angle*.

The Higgs potential is as general as possible if it contains all possible quadratic and quartic couplings. Odd order terms cannot be included as it would break the symmetry present and higher order even terms are excluded to make the theory renormalizable. Writing the Higgs potential in the *generic basis*, where Φ_1 and Φ_2 are the Higgs doublets above, it is

$$\begin{aligned} V(\Phi_1, \Phi_2) = {} & m_{11}^2 \Phi_1^\dagger \Phi_1 + m_{22}^2 \Phi_2^\dagger \Phi_2 - (m_{12}^2 \Phi_1^\dagger \Phi_2 + h.c.) + \frac{1}{2}\lambda_1 (\Phi_1^\dagger \Phi_1)^2 \\ & + \frac{1}{2}\lambda_2 (\Phi_2^\dagger \Phi_2)^2 + \lambda_3 (\Phi_1^\dagger \Phi_1)(\Phi_2^\dagger \Phi_2) + \lambda_4 (\Phi_1^\dagger \Phi_2)(\Phi_2^\dagger \Phi_1) \\ & + \left[\frac{1}{2}\lambda_5 (\Phi_1^\dagger \Phi_2)^2 + \lambda_6 (\Phi_1^\dagger \Phi_1)(\Phi_1^\dagger \Phi_2) + \lambda_7 (\Phi_2^\dagger \Phi_2)(\Phi_1^\dagger \Phi_2) + h.c. \right], \end{aligned} \tag{4}$$

where h.c. refers to the hermitian conjugate, m_{ij}^2 are the quadratic couplings and λ_i are the quartic couplings. It is possible for the couplings m_{12}^2, λ_5, λ_6 and λ_7 to be complex while the other couplings are strictly real.

The 2HDM is $\mathbb{Z}_2$ symmetric if Eq.4 is invariant under the transformation

$$\Phi_1 \longrightarrow +\Phi_1, \Phi_2 \longrightarrow -\Phi_2. \tag{5}$$

Φ is now no longer generic but rather the specific basis for which Eq.5 holds, which leads to the condition that $m_{12}^2 = \lambda_6 = \lambda_7 = 0$. The symmetry has the effect that no flavour-changing neutral currents (FCNC) are allowed in the theory [14]. The $\mathbb{Z}_2$ symmetry is said to be *softly broken* if $m_{12} \neq 0$ while $\lambda_6 = \lambda_7 = 0$. The argument for the softly broken symmetry is that the FCNC will be suppressed as a result of it, in order to satisfy the experimental constraints from FCNC.

The vacuum expectation values (VEVs), v_i, of the doublets in the generic basis are defined to be

$$\langle \Phi_i \rangle = \frac{v_i}{\sqrt{2}} \begin{pmatrix} 0 \\ 1 \end{pmatrix}, (i = 1, 2), \tag{6}$$

where v is the magnitude

$$v^2 = v_1^2 + v_2^2. \tag{7}$$

It follows that v has the same magnitude as the VEV from the Standard Model such that the mass of the $W^{\pm}$ and Z boson are the same as in the SM. From the VEVs an angle β can be defined as

$$\tan(\beta) = \frac{v_2}{v_1}. \tag{8}$$

Going forward an abbreviated notation for the trigonometric functions will be used where

$$t_\beta = \tan(\beta),\ c_\beta = \cos(\beta),\ s_\beta = \sin(\beta). \tag{9}$$

Using the angle β one can define the *Higgs basis* as the doublets resulting from a rotation of Φ by the angle β. With the VEVs of the Higgs basis having the property

$$\langle H_1 \rangle = \frac{v}{\sqrt{2}} \begin{pmatrix} 0 \\ 1 \end{pmatrix}, \langle H_2 \rangle = 0, \tag{10}$$

where H_i are the Higgs doublets in the Higgs basis and v is the VEV from the SM. As these Higgs doublets are the result of a rotation by β they can be written as

$$\begin{pmatrix} H_1 \\ H_2 \end{pmatrix} = \begin{pmatrix} c_\beta & s_\beta \\ -s_\beta & c_\beta \end{pmatrix} \begin{pmatrix} \Phi_1 \\ \Phi_2 \end{pmatrix}. \tag{11}$$

The VEV, in Eq.10, makes the Higgs basis an interesting choice of basis as H_1 will be similar to the SM doublet in which case H_2 can be interpreted as an extension to the SM.

The Higgs potential written in the Higgs basis is

$$\begin{aligned} V(H_1,H_2) = {} & Y_1 H_1^\dagger H_1 + Y_2 H_2^\dagger H_2 + (Y_3 H_1^\dagger H_2 + h.c.) + \frac{1}{2} Z_1 (H_1^\dagger H_1)^2 \\ & + \frac{1}{2} Z_2 (H_2^\dagger H_2)^2 + Z_3 (H_1^\dagger H_1)(H_2^\dagger H_2) + Z_4 (H_1^\dagger H_2)(H_2^\dagger H_1) \\ & + \left[\frac{1}{2} Z_5 (H_1^\dagger H_2)^2 + Z_6 (H_1^\dagger H_1)(H_1^\dagger H_2) + Z_7 (H_2^\dagger H_2)(H_1^\dagger H_2) + h.c. \right]. \end{aligned} \tag{12}$$

The quadratic couplings, Y_i, and quartic couplings, Z_i, in the Higgs basis can be calculated from the couplings in the generic basis, m_{ij} and λ_i. This entails that there is an transformation between the Higgs basis couplings and the generic basis couplings [15], the formulas for doing this transformation are collected in appendix A. Using the potential in the Higgs basis, the mass matrix can be calculated which results in the following masses

$$m_{H^\pm}^2 = Y_2 + \frac{v^2}{2} Z_3, \tag{13}$$

$$m_A^2 = Y_2 + \frac{v^2}{2} (Z_3 + Z_4 - Z_5), \tag{14}$$

$$m_{H/h}^2 = \frac{1}{2} \left(m_A^2 + (Z_1 + Z_5) v^2 \pm \sqrt{[m_A^2 + (Z_5 - Z_1) v^2]^2 + 4 Z_6^2 v^4} \right). \tag{15}$$

These formulas assumes a CP-conserving model with real couplings.

While the $\mathbb{Z}_2$-symmetric theory has no CP breaking the softly-broken theory can have it. However this paper will only concern itself with the case when the couplings in Eq.12 are real which means that CP is not broken as a result of the 2HDM. While taking the couplings as real parameters is sufficient for conserving CP there are weaker conditions which will also conserve CP [9].

2.2 Theoretical Constraints on the 2HDM

The theoretical constraints of unitarity and stability are imposed on the theory, therefore the conditions for both are needed. A more detailed discussion of the unitary constraints can be found in [16] and of the stability constraints in [17].

Within a unitary theory the scattering matrices preserve inner products which is important as the magnitude of inner products are interpreted as probabilities. Finding the conditions for the 2HDM to be unitary involves four of these scattering matrices. These

matrices are [16]

$$\Lambda_{21} = \begin{bmatrix} \lambda_1 & \lambda_5 & \sqrt{2}\lambda_6 \\ \lambda_5^* & \lambda_2 & \sqrt{2}\lambda_7^* \\ \sqrt{2}\lambda_6^* & \sqrt{2}\lambda_7 & \lambda_3+\lambda_4 \end{bmatrix}, \tag{16}$$

$$\Lambda_{20} = \lambda_3 - \lambda_4, \tag{17}$$

$$\Lambda_{01} = \begin{bmatrix} \lambda_1 & \lambda_4 & \lambda_6 & \lambda_6^* \\ \lambda_4 & \lambda_2 & \lambda_7 & \lambda_7^* \\ \lambda_6^* & \lambda_7^* & \lambda_3 & \lambda_5^* \\ \lambda_6 & \lambda_7 & \lambda_5 & \lambda_3 \end{bmatrix}, \tag{18}$$

$$\Lambda_{00} = \begin{bmatrix} 3\lambda_1 & 2\lambda_3+\lambda_4 & 3\lambda_6 & 3\lambda_6^* \\ 2\lambda_3+\lambda_4 & 3\lambda_2 & 3\lambda_7 & 3\lambda_7^* \\ 3\lambda_6^* & 3\lambda_7^* & \lambda_3+2\lambda_4 & 3\lambda_5^* \\ 3\lambda_6 & 3\lambda_7 & 3\lambda_5 & \lambda_3+2\lambda_4 \end{bmatrix}. \tag{19}$$

Labeling the eigenvalues of the scattering matrices as Λ_i then the unitarity constraint, on tree-level, is fulfilled if all eigenvalues follow [16]

$$\Lambda_i < 8\pi. \tag{20}$$

Having a Higgs potential that is bounded from below is referred to as stability which makes it possible for the VEV to be a global minimum. To ensure stability the properties of another matrix is investigated. For a model with softly broken $\mathbb{Z}_2$ symmetry this matrix is [17]

$$\Lambda = \frac{1}{2}\begin{bmatrix} \frac{1}{2}(Z_1+Z_2)+Z_3 & -Z_6-Z_7 & 0 & -\frac{1}{2}(Z_1-Z_2) \\ Z_6+Z_7 & -Z_4-Z_5 & 0 & -Z_6+Z_7 \\ 0 & 0 & -Z_4+Z_5 & 0 \\ \frac{1}{2}(Z_1-Z_2) & -Z_6+Z_7 & 0 & -\frac{1}{2}(Z_1+Z_2)+Z_3 \end{bmatrix}. \tag{21}$$

The stability condition is fulfilled if all the following conditions are met [17]:

1. all the eigenvalues of Λ are real,
2. the largest eigenvalue of Λ is positive,
3. there are four linearly independent eigenvectors of Λ each corresponding to an eigenvalue,
4. the eigenvector corresponding to the largest eigenvector is timelike while the other eigenvectors are spacelike.

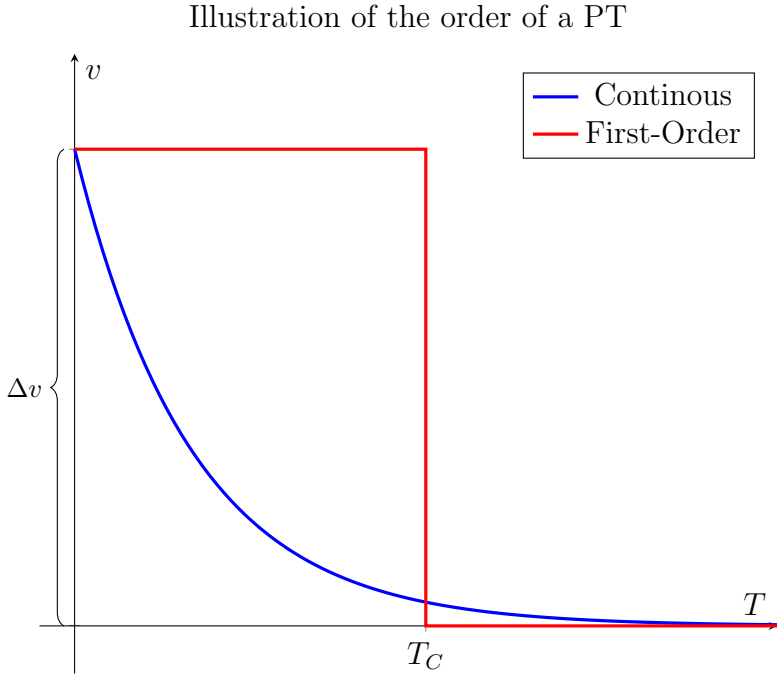

Figure 1: Two phase transitions of different order that showcase the difference between first-order PTs and other PTs. The red graph is the first-order change in VEV, v, while the blue is the non first-order change in VEV as a function of temperature, T.

2.3 Phase Transition

The critical temperature, T_C, of an EWPT is defined as the temperature where there are two minima in the Higgs potential with equal value. In order for this phase transition to be the cause of baryogenesis it needs to be a *strong first-order* phase transition [2]. An EWPT being first-order means that the change in VEV occurs abruptly at T_C, as illustrated in fig. 1. Contrary to first-order phase transitions, the second-order phase transitions occur continuously over a range of temperatures. The first-order phase transition is also *strong* if the change in vacuum expectation value is large in comparison to the critical temperature [3]. More quantitatively, the ratio $\xi = \frac{\Delta v}{T_C}$ is used and the phase transition is considered strong if the condition

$$\xi = \frac{\Delta v}{T_C} \geq 1, \tag{22}$$

holds.

The breaking of the electroweak symmetry occurs through a PT. This means that at high temperatures the Higgs potential is symmetric around the origin and the origin is a global minimum. This high temperature potential is illustrated in the one-dimensional case by the $T > T_C$ curve in fig. 2. Also illustrated is the potential when the temperature is lowered and the potential stops having a single minimum and gains a VEV. At the critical temperature two or more minima are equal in value by the definition of the critical

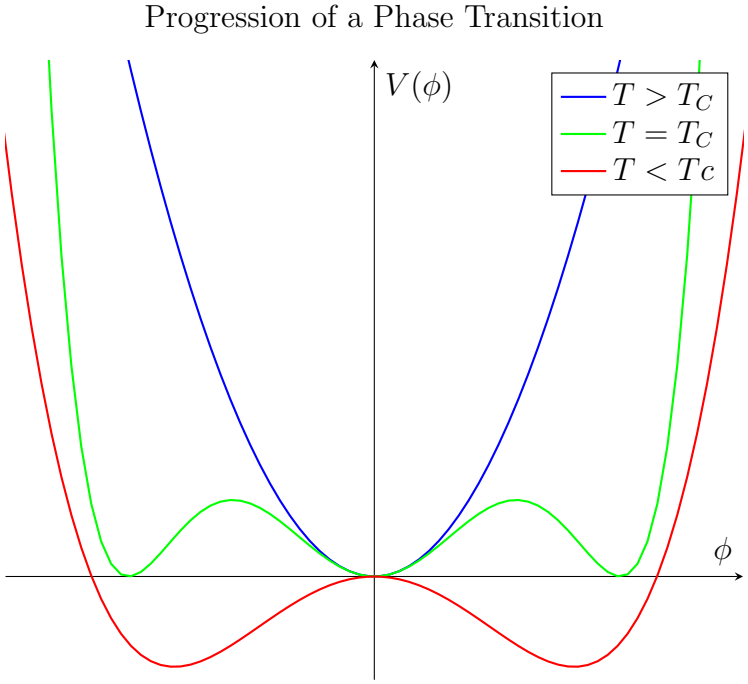

Figure 2: Illustration of the potential for different temperature relevant to a PT in the one dimensional case.

temperature which leads to the potential $T = T_C$ in the figure. When the temperature is sufficiently low this results in a "Mexican hat potential" which is still symmetric around the origin but there are now multiple minima, this is illustrated in $T < T_C$ in fig. 2.

Allowing for quantum tunneling a system can go from one state to another even if there is not sufficient energy to overcome the potential barrier between the states. This allows for situations where particles go from one minima to another minima in the Higgs potential. This means that when several "phases" are present, which will occur around T_C but not necessarily only at T_C, bubbles can form. Bubbles are regions of space where the "new" phase is present in a stable manner. An example of this would be in the early universe when the Higgs potential gained a VEV. When the universe expanded and therefore cooled bubbles of the new metastable phase formed. These bubbles can then collapse, expand and even collide with one another depending on the conditions. As the temperature was further lowered in the universe, the bubbles become more likely to expand until, finally, the universe is encompassed by the new phase.

2.4 Dimensional Reduction

The dimensional reduction that is used by programs such as DRalgo includes an effective field theory that takes into account the thermal aspects of the full field theory. An effective field theory entails going from a general four-dimensional Lagrangian with all available fields to a less general three dimensional Lagrangian with fewer fields. The dimension that

is removed is the time-dimension which can be done since the temperature is added as a degree of freedom. If a system is in thermal equilibrium there is only one temperature T in the system at a time t. Much of the information about the time is then contained in the temperature which allows for the removal of the time dimension in the reduced theory. This new reduced Lagrangian does however fulfill all symmetries present at higher temperatures making it a good approximation there [6]. Using this effective field theory several parts of the Lagrangian can be *integrated out* such that the new Lagrangian is only 3D. The fields that can be integrated out are the fields that have a higher energy scale than the scale of the problem that is being examined. If, at a temperature scale T, the energy of some field is far higher than that scale then the field can be integrated out from the Lagrangian. This new theory, that has parts integrated out, is in turn simpler and therefore it is easier to calculate temperature dependent effects such as phase transitions in that theory. From this one can *match* the results of the dimensionally reduced theory to the original 4D theory if the temperature is sufficiently large [18]. The temperature scale that this *matching* is done at is denoted as the *matching scale*, μ.

The steps involved in dimensional reduction can be performed differently dependent on the order of the theory. In DRalgo there is the leading order (LO) dimensional reduction and the next-to-leading order (NLO) dimensional reduction. The potential of the model can also be taken as LO or NLO which corresponds to a potential including only tree-level in the LO case contributions or also including one-loop contributions in the NLO case [7]. This is different to the order of the dimensional reduction which impacts how the dimensional reduction itself is performed. The NLO dimensional reduction will have certain higher-order corrections taken into account in comparison to the LO dimensional reduction. An example of this is the calculation of the masses in the 4D theory which is required for the matching. For this the LO case only require these to be calculated using Feynman diagrams at the 1-loop level while the NLO case requires also the 2-loop level diagrams.

The dimensional reduction follows a procedure that will be covered in a condensed manner here following Ref.[18]. Firstly, the 4D temperature dependent theory is set-up and evolved to a matching scale of

$$\mu = C\pi T, \tag{23}$$

where C is a dimensionless constant that should be around 1. However a small change in C should still keep the theory the same if πT is large enough as is required by the theory. πT is required to be larger than the masses of the bosons for dimensional reduction to be used. At these temperature scales the theories are *matched* meaning that calculations can be performed in the 4D to get information about the temperature dependent properties of the 3D theory. These calculations can be performed at one-loop level, in the LO case, or at two-loop level, in the NLO case. This will involve integrating over the contributions of certain fields which makes those fields disappear. The fields integrated over are the modes of the fields for which the energy scale is larger than the temperature scale. These high energy modes corresponds to the *hard scale* energy regime and integrating these out leads

to a theory in the *soft* energy regime.

The theory in the soft energy regime can be further reduced to the *ultrasoft regime*. To further reduce the theory to the ultrasoft scale one can integrate out more fields. At the soft scale the theory is 3D meaning that the time dimension is removed from the theory due to thermal effects. To compensate for this there are new temporal fields, these come about when the time dimension is removed, that represent the impact of time. These fields are said to be of energy scale $E \sim gT$, where g is the gauge coupling. In the ultrasoft scale all fields in the energy regime $E \sim gT$ are integrated out including the temporal fields. This creates a theory that is as reduced as possible and using the potential of it PTs can be found that should match the PTs of the initial 4D theory.

3 Parametrizations

In this section the parametrization of the 2HDM is presented. In section 3.1 the hybrid basis is introduced and the parameters used to define the model. Furthermore in section 3.2 it is explained how to convert from a parametrization containing the masses of the particles in 2HDM to the hybrid basis.

3.1 The Hybrid Basis

A parametrization of the 2HDM gives a set of variables such that the couplings of the Higgs potential, m and λ in Eq.4 , are uniquely determined. In a model with a softly broken $\mathbb{Z}_2$ symmetry, where $\lambda_6 = \lambda_7 = 0$, there are 7 required parameters, if all are real, in order to uniquely determine the couplings. This is due to the fact that there are 8 couplings and one angle β that need to be determined, assuming v is the same value as the VEV in the Standard Model. This number is then reduced to 7 through the two tadpole equations. These are defined by the criteria

$$\left.\frac{\partial V(\Phi_1, \Phi_2)}{\partial \Phi_i}\right|_{\Phi_i = <\Phi_i>} = 0, \tag{24}$$

which follows from the minimization criteria at the vacuum expectation values.

The hybrid basis, introduced in [9], uses the following parameters

$$m_h, m_H, c_{\beta-\alpha}, t_\beta, Z_4, Z_5, Z_7, \tag{25}$$

as a parametrization. This basis is useful as m_h can be taken as the mass of the Standard Model Higgs particle to match experiment. In addition, the coupling of H to the W and Z bosons depends on $c_{\beta-\alpha}$ [9]. This means that taking small values for $c_{\beta-\alpha}$ leads to a weak coupling to the non-SM Higgs. The values of the Z-couplings can vary but need to be kept small ($|Z_i| \lesssim 4\pi$) in order for the model to be able to be unitary and stable at tree-level. The Hybrid basis thus provides parameters which has some useful properties to construct a 2HDM model.

The quartic couplings of the Higgs basis can be obtained from the Hybrid parametrization as [11]

$$Z_1 = \frac{m_h^2}{v^2} s_{\beta-\alpha}, \tag{26}$$

$$Z_6 = \frac{m_h^2 - m_H^2}{v^2} c_{\beta-\alpha} s_{\beta-\alpha}., \tag{27}$$

$$Z_2 = Z_1 + 2(Z_6 + Z_7)\cot(2\beta), \tag{28}$$

$$Z_3 = Z_1 - Z_4 - Z_5 + 2Z_6\cot(2\beta) - (Z_6 - Z_7)t_{2\beta}. \tag{29}$$

The tadpole equations give Y_1 and Y_3 as

$$Y_1 = -\frac{1}{2} Z_1 v^2, \tag{30}$$

$$Y_3 = -\frac{1}{2} Z_6 v^2, \tag{31}$$

which follows from the minimization condition in the Higgs basis, Eq.24 but expressed in the Higgs basis. The relation of the mass of A, the CP-odd particle, from Eqs.14-15 results in

$$\begin{cases} m_A^2 & = Y_2 + \frac{1}{2}(Z_3 + Z_4 - Z_5)v^2 \\ m_A^2 + Z_5 v^2 & = m_H^2 s_{\beta-\alpha}^2 + m_h^2 c_{\beta-\alpha}^2 \end{cases} \tag{32}$$

$$\implies Y_2 = m_H^2 s_{\beta-\alpha}^2 + m_h^2 c_{\beta-\alpha}^2 - \frac{1}{2}(Z_3 + Z_4 + Z_5)v^2, \tag{33}$$

which allows for the calculation of Y_2. Thus from Eqs.26-33 all the quadratic and quartic couplings in the Higgs basis can be calculated from the hybrid basis.

The quadratic, m_{ij}^2, and quartic couplings, λ_i, in the generic basis are also of interest. These can be obtained, as discussed earlier, from the couplings in the Higgs basis. In the case where the couplings in the Higgs basis are chosen to be real and with a softly broken $\mathbb{Z}_2$ symmetry the formulas for these conversions are the ones presented in appendix A.

3.2 The Mass Basis

At times, working with parametrizations other than the hybrid basis is useful especially for comparisons to previous results. One such other parametrization is the one which uses the masses, a *mass basis*. This basis uses the parameters

$$c_{\beta-\alpha}, t_\beta, m_h, m_H, m_A, m_{H^\pm}, m_{12}^2.$$

It is possible to convert from this set of parameters to the hybrid basis. This is done by converting $m_A, m_{H^\pm}, m_{12}^2$ to Z_4, Z_5, Z_7.

The procedure of the conversion from the mass basis starts with calculating Z_5. From Eq.15 the Z_5 coupling in the hybrid basis can be calculated as

$$Z_5 v^2 = m_H^2 s_{\beta-\alpha}^2 + m_h^2 c_{\beta-\alpha}^2 - m_A^2. \tag{34}$$

In addition, from the mass of the charged Higgs particle the Z_4 coupling can be calculated. It is given by the difference of mass between $H^{\pm}$ and m_A , from Eqs.13-14, resulting in

$$Z_4 = Z_5 + \frac{2(m_A^2 - m_{H^{\pm}}^2)}{v^2}. \tag{35}$$

From m_{12}^2 and all of the known particle masses the last Z coupling in the hybrid basis can be calculated. This is done by using the relation [11]

$$Z_7 = Z_6 + \frac{2\cot(2\beta)}{v^2}(m_H^2 s_{\beta-\alpha}^2 + m_h^2 c_{\beta-\alpha}^2 - \frac{m_{12}^2}{c_\beta s_\beta}), \tag{36}$$

where Z_6 is obtained from Eq.27. Using Eqs.34-36 the conversion from the parameters in the mass basis to the parameters in the hybrid basis can be done.

4 Numerical methods

To simulate phase transitions the packages *CosmoTransitions* [10] and *DRalgo* [7] are used. DRalgo uses *GroupMath* [19] to be able to define a generic model for which the dimensional reduction method can be used. Using DRalgo a 2HDM model is defined and then that model is used by CosmoTransitions to find phase transitions. The export of the model from DRalgo and applying this model in CosmoTransitions was accomplished using a package written by Mårten Bertenstam [20].

Using the model defined by DRalgo, CosmoTransitions finds the phase transitions from the potential of the model by varying the temperature. It accomplishes this by tracking the minima of the potential over a range of temperatures. When there is the possibility for a particle to go from being in the region of one minimum to the region of another, this is called a *bubble*. CosmoTransitions investigates phase transitions by first finding a direct path between two minima and then deforming that path to find the ideal path, the path that extremizes the action. It uses this information to, given a potential with temperature dependence, find if a phase transition occurs and if so what the critical temperature is [10].

The code written for this project uses the 7 parameters in the hybrid basis to create a model defined from DRalgo using the export code. In order to do this the 7 parameters from the hybrid basis need to be converted to the λ and m couplings. This is done by using Eqs.26-33 to obtain all couplings in the Higgs basis. After this Eqs.38-45 are used to convert to the generic basis which are the parameters required to define the DRalgo model used for Cosmotransitions. After this the model is defined by the export code and used by CosmoTransitions to find the potential PTs and critical temperatures. At this step ξ is calculated and if there are multiple PTs the one with the highest ξ is used and the others are discarded, transitions which are not identified as first-order by CosmoTransitions are also discarded.

Using this set-up a parameter point is given to the code which then outputs a value of ξ and T_C. Building on this several parameter points can be passed through and the results are stored in text files alongside the parameters themselves which allows for plotting the results in different ways.

Table 1: Parameter bounds or values for the parameter search and the distribution used. A logarithmic distribution means that the logarithm of the distribution would be uniformly distributed.

Parameter	m_h(GeV)	m_H(GeV)	m_A(GeV)	$m_{H^\pm}$(GeV)	m_{12}^2 (GeV^2)	$c_{\beta-\alpha}$	t_β
Bounds	125	130...1000	65...1000	65...1000	0...5·10^5	-0.1...0.1	1...35
Distribution	Fixed	Uniform	Uniform	Uniform	Log	Uniform	Log

5 Numerical results

A search varying the parameters m_H, m_A, $m_{H^\pm}$, m_{12}^2, $c_{\beta-\alpha}$ and t_β is done. These parameters are chosen to match a search done in [9]. The values used for the bounds as well as the type of distribution used to vary the different quantities is presented in table 1. For most parameters uniform distributions are used but when the parameter spans several orders of magnitudes another type of distribution is used. This distribution is denoted "log" and is chosen such that the logarithm of the distribution is uniformly distributed. A search through the parameter space is done by randomly selecting points within the bounds and in accordance to the distribution laid out in table 1. This search is done for 100 000 randomly chosen unitary and stable points.

Using this method a search through the parameter space is done for both the NLO and LO models for randomly chosen points. These random points are the same for both the LO and NLO case. The results of these are plotted in fig. 3a for the NLO case and fig. 3b for the LO case. The points with phase transitions that are not classified as first order by CosmoTransitions are discarded. In addition to this, the ones that are first-order but not strong ($\xi < 1$) are plotted as grey points in the background.

The NLO search found several points with strong first-order phase transitions. This is represented in fig. 3a as colored points were each point represents a PT and the color represents ξ. From the figure it is clear that for larger values of m_H there are PT however they are not strong. There are also regions of the parameter space which seemingly lacks any first-order PT. For example when m_A or m_H is sufficiently large there are regions of white space in the plot which represents no found first-order PT even though the area was searched. The largest amount of strong first-order PT occurred in the region

$$130 \text{ GeV} \lesssim m_H \lesssim 400 \text{ GeV} \quad , \quad 65 \text{ GeV} \lesssim m_A \lesssim 500 \text{ GeV}. \tag{37}$$

This is different from the LO search, shown in fig. 3b in a similar manner as the NLO plot, where the points with strong PT are more spread out than the NLO case. The LO search also lacks the region of PT that are not strong but are first-order that the NLO case has, this is around $m_H \approx 800$ GeV. However the maximum value of ξ found for both models is quite similar, $\xi \approx 13$. As mentioned, the LO model produces strong PTs in a larger area than the NLO model which results in there being some regions where, in the NLO model, no strong PTs were found but there are strong PTs in the LO case. Specifically for $m_A \gtrsim 400$ GeV, $m_H \gtrsim 300$ GeV this feature is clear from the plot.

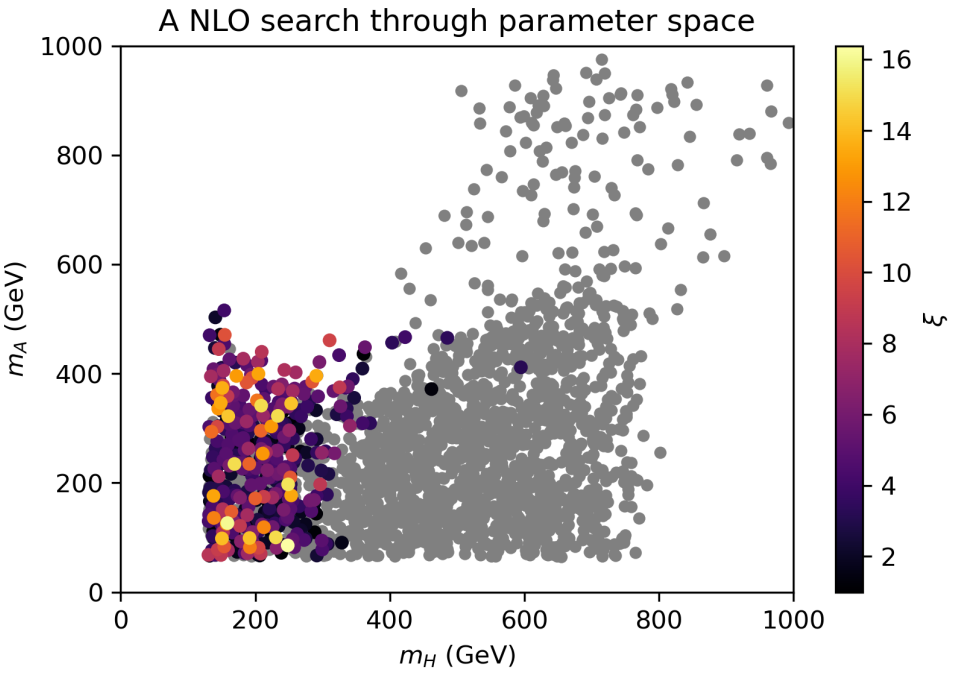

(a) Next-to-leading order search

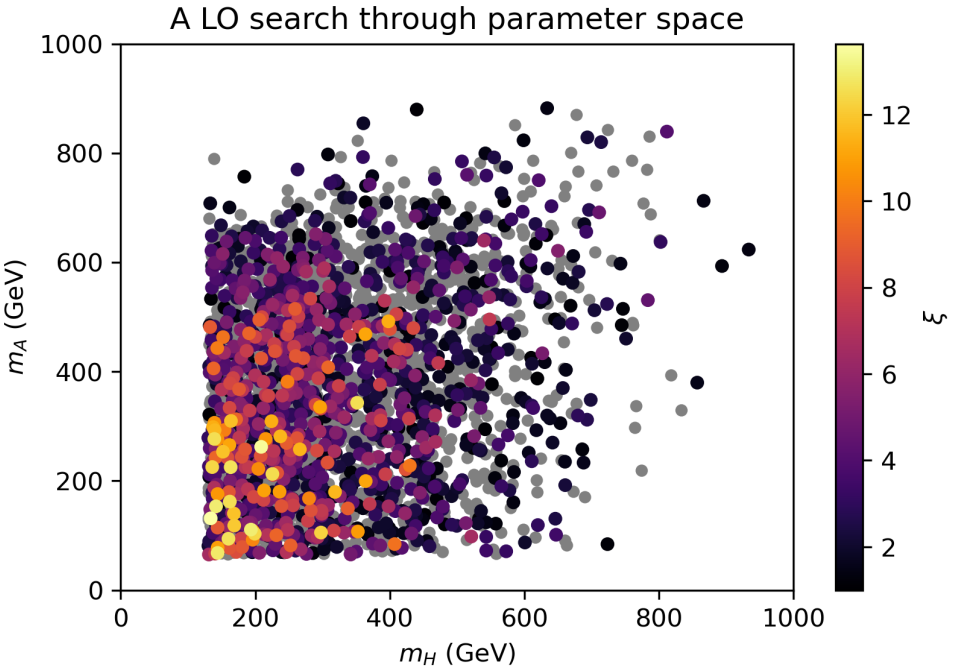

(b) Leading order search

Figure 3: A next-to-leading order(a) and leading order(b) search where several parameters were varied randomly according to table 1 and points with a first-order PT were found. It is the projection of this search onto the $m_H m_A$ plane that is shown. The color represents the strength of the PT and "greyed-out" points are points where the PT is not strong but is first-order.

Table 2: Parameter bounds or values for the second parameter search. All distributions used for random selection of parameters are uniform distributions.

m_h(GeV)	m_H(GeV)	m_A(GeV)	$m_{H^\pm}$(GeV)	m_{12}^2 (GeV^2)	α	t_β
125	130...1000	65...1000	65...1000	0...5·10^5	$-\frac{\pi}{2}...\frac{\pi}{2}$	1...35

Neither figure 3a nor figure 3b has a great similarity to the results in [8] which varies similar parameters. A possible explanation to this is the way the sampling is done, the distributions used could impact the resulting plots. Therefore a similar search is done but this time using the parameters in table 2. These parameters are a more close match to what was done in the previous paper. For the same reason all distributions are chosen to be uniform.

Using this parameter set, the search is done at both LO and NLO, using the same set of points for the LO search and the NLO search. This set contained 100 000 points that are unitary and stable at tree-level. The same set was used for the LO and NLO to better compare the results for between orders. Moreover, two different values for the C parameter are chosen, the parameter that determines the matching scale in Eq.23. For the previous searches C was kept at 1 as the matching scale was not of interest in those searches. As previously done, the PTs that are not strong are represented by grey points and all points in the plot are identified as first-order by CosmoTransitions.

The search done for the plot in figure 4a is done at NLO and C is kept at 1, the same value as previous searches. There are similarities to figure 3a as the parameters varied are very similar. The only differences are that α is being varied as opposed to previously varying $c_{\beta-\alpha}$ and the distributions used. α is being varied more freely than $c_{\beta-\alpha}$ which could explain some of the differences between the plots. Differences such as seeing more PTs for large values of m_H and m_A (m_H,$m_A > 600$) than what was previously there. However, overall the change in parameters did not have a large impact on the result. The region that contains strong PTs is still largely the same as previously, it is still confined to the region defined by Eq.37.

Both the searches shown in fig. 3a and fig. 4a closely resemble the search done in [8], which used a different method, in terms of how the sampling was done. However, the results here are quite dissimilar to the previous search, which could be due to flaws in either of the methods. It could be that the points of interest in [8] have phase transitions that is outside the temperature range described by dimensional reduction.

Using the same set of points as the search in fig. 4a a search is done using $C = 1/2$. This amounts to lowering the matching scale to see the impact of it. The resulting plot, presented in fig. 4b, has a region of strong PTs that is less spread out than the $C = 1$ case and seemingly has a smaller region with a large value of ξ ($\xi \gtrsim 10$). The $C = 1/2$ case also does not have the same number of points in the region of PTs that are not strong as in the $C = 1$ case, this region is a lot sparser in the $C = 1/2$ case. Doing this same search for the $C = 2$ case the resulting time it took to generate the PTs using CosmoTransitions was far greater than for the other cases of C. Therefore, this report is limited to the $C = 1/2$ and

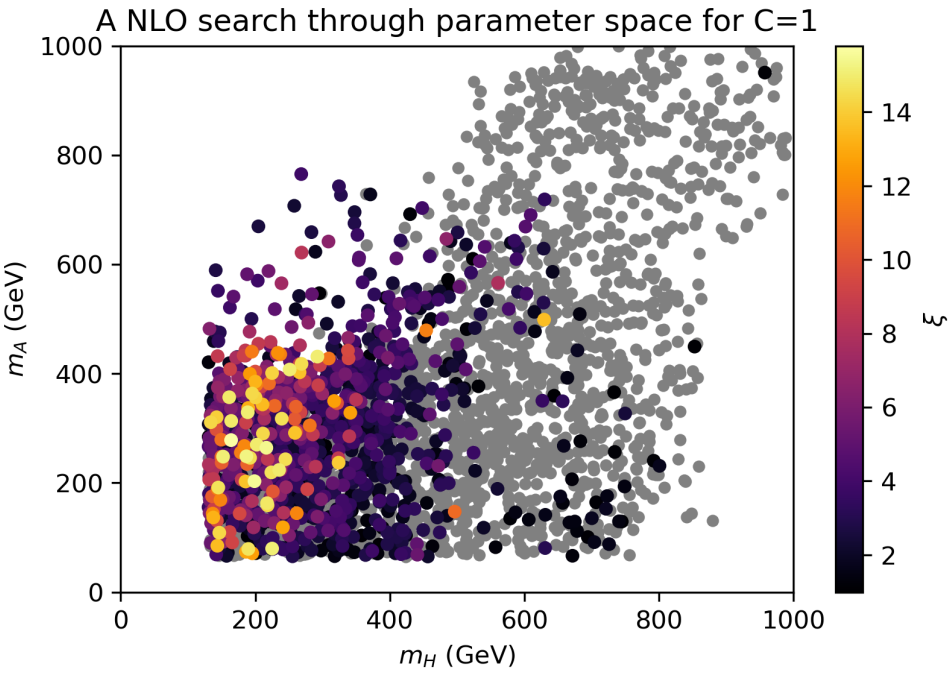

(a) Search using $C = 1$

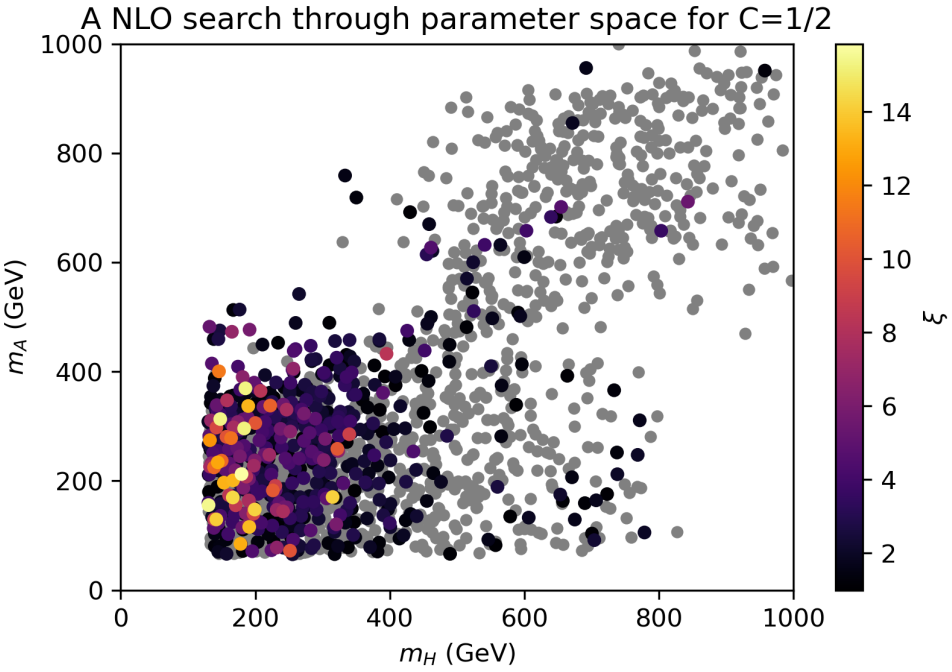

(b) Search using $C = 1/2$

Figure 4: Random search done at NLO which uses uniform distributions, parameters given in table 2. The search was done using two different values of C. The color of the points indicate the strength of the PT and grey points represent a PT that is first-order but not strong.

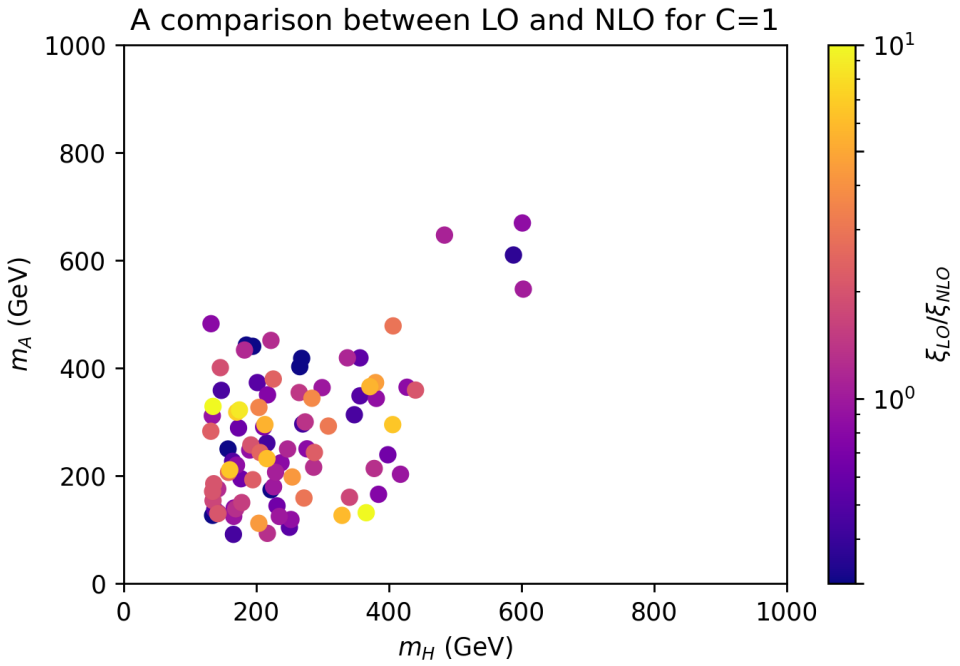

Figure 5: Comparison done between the LO and NLO strength by showing the ratio between the two as the color of the points. This was done at $C = 1$.

$C = 1$ cases.

The order of the model was investigated for the matching scale at $C = 1$. This was done by repeating the search that was done for the results at NLO in fig. 4a but at LO. For each point where both the NLO search and the LO search yielded a strong PT a comparison is done, taking $\frac{\xi_{LO}}{\xi_{NLO}}$ as the comparison. The results are shown in fig. 5.

Figure 5 shows that the agreement between the LO and NLO search varies significantly from point to point. In some points they differ by as much as a factor of 10 while other points appear to match well between orders. All points that were chosen were strong (meaning $\xi > 1$) at both LO and NLO which makes a factor of 10 a significant difference between orders. This significant difference occurs for several points which showcases the importance of order.

Another pattern that is found in this comparison is that there are far more points in the NLO order search than in this plot. This is a result of the LO search not always being able to find a strong PT were the NLO search can. The reverse can also occur were the LO search finds a strong PT that is not present at higher order. All this showcases the impact that order has on the results, meaning that searches should be performed at least at NLO.

In order to more explicitly see the dependence on matching scale, plots were done that show how ξ changes with C for specific points in parameter space. The points used are presented in table 3 with a name for each specific scenario. For each parameter point the model was defined using many different values of C and finding the strongest PT for each

Table 3: The parameters of different scenarios. These scenarios are then investigated by varying the matching scale.

Scenario	m_h(GeV)	m_H(GeV)	$c_{\beta-\alpha}$	t_β	Z_4	Z_5	Z_7
Split	125	250	0.98	1.37	0.29	0.10	-0.26
Decrease	125	314	0.48	4.6	4.4	-2.0	-0.57

value. This means that it is only the highest value of ξ, for every value of C, that is present in these graphs. This results in the plots that show the dependence on matching scale in fig. 6. The value of the critical temperature for the found PT is also presented as the color of the point, if a point does not have a PT the point is red.

For the split scenario in fig. 6a there is a clear dependence on the matching scale. It is only for some values that the PT at $\xi \approx 6$ is found while other times the only PT it is able to find is at $\xi \approx 2$. As only the PT with the highest value of ξ is used this means that a slight variation in the matching scale could, at least for this point, have a large effect on the results.

In contrast to fig. 6a, fig. 6b shows the decrease scenario with a more continuous decrease in ξ until no PT is found. This shows a clear relationship between ξ and C where ξ is smaller for larger values of C. However, T_C decreases for larger values of C which means that the decrease in ξ comes from changes in the VEVs. This, in turn, means that the structure of the phases depend on the matching scale which means that the theory is likely not valid in this case.

Both fig. 6a and 6b shows flaws in the dependence of the results on the matching scale. This could be due to the critical temperature being low which means that the theory behind dimensional reduction no longer holds.

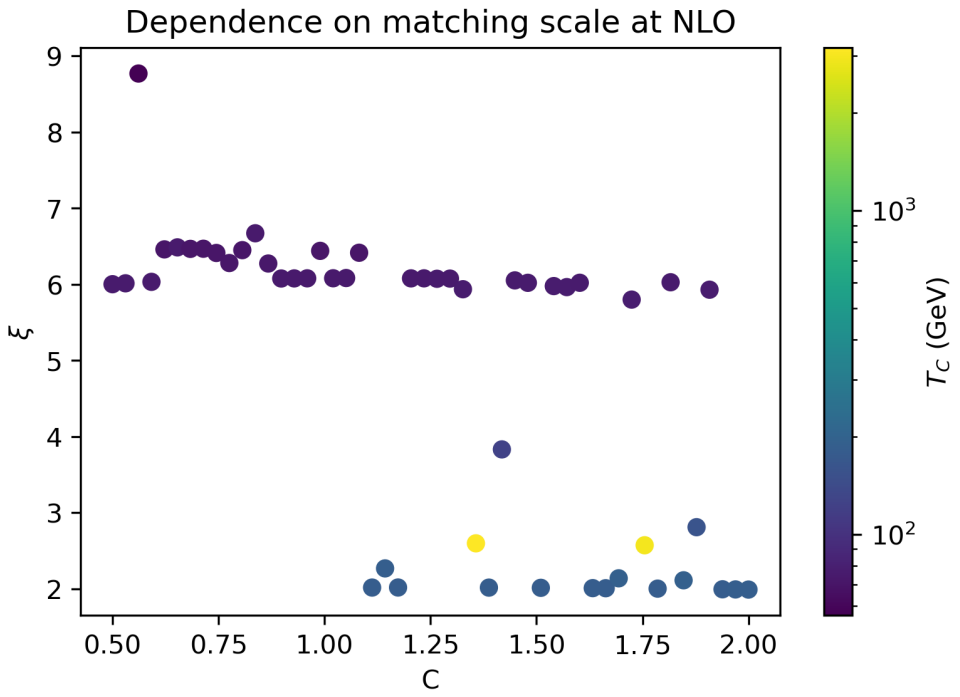

(a) Comparison for the *split* scenario

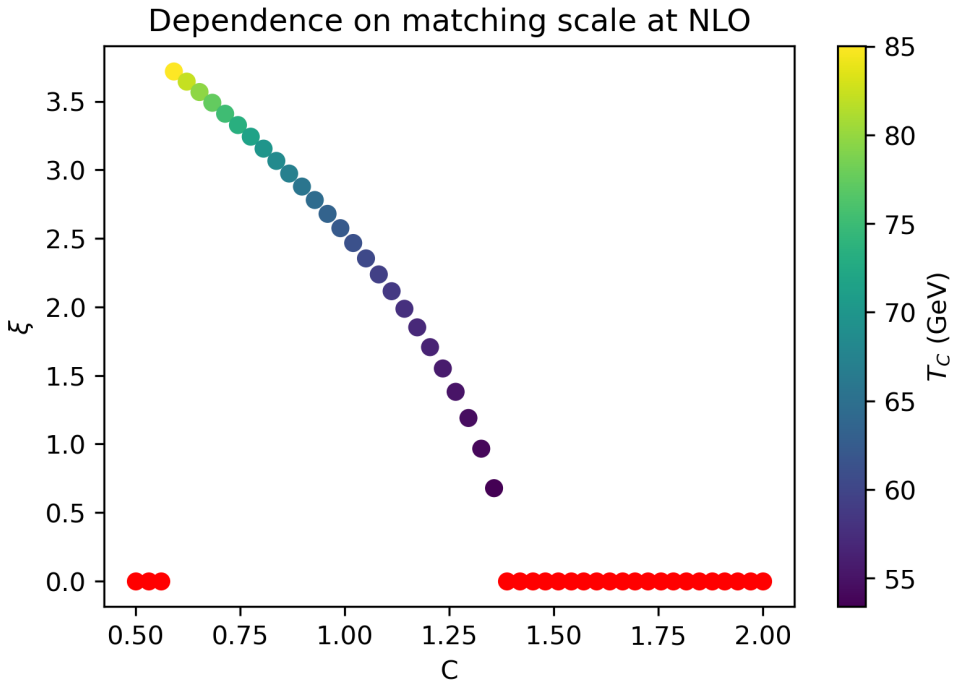

(b) Comparison for the *decrease* scenario

Figure 6: Plotting the strength of the phase transition, ξ against the matching scale parameter,C, at next-to-leading order using the parameters specified by the scenario. The color of the points represents the critical temperature.

6 Conclusion

In summary, dimensional reduction was used to study the temperature dependence of the effective potential for a CP-conserving 2HDM with a softly broken $\mathbb{Z}_2$ symmetry. Seven parameters were used to uniquely determine the necessary couplings in the model. This was then used to find PTs which in turn could be classified by strength and order. Using this, searches were performed and the impact that internal parameters of the method have on the results was investigated, specifically matching scale and order was examined.

Various searches were done in the parameter space in an attempt to find strong PTs using different distributions and parameters that were varied. The varied parameters were partially inspired by the set used in Ref.[8], where a similar search was done but using a different method. However, the results do not match for the different methods when comparing to the previous results. This leads to an examination of how the model used holds up, which is done by comparing how results change with order or matching scale. How much the results changed between next-to-leading order and leading order varied significantly, some points differing by a factor of 10 while other points match well. Similar results are found for the specific points where the impact of the matching scale was examined, the strength of the PT was strongly affected by the change in matching scale. This all showcases potential flaws in the method used.

The problem with the dependence of the strength on the matching scale could be due to the low temperature of the phase transitions examined. Ideally, the strength, ξ, would not depend on C in the ranges examined for the model to be valid. This could be an indication of a breakdown of the validity of the model, with such low critical temperatures the dimensional reduction method may not be applicable. An interesting investigation would be to see how the results change if you include some type of limit on the PTs that are looked at in order to avoid these issues. This could be done by ignoring PTs that have a critical temperature below a certain threshold or other ways of ensuring that the dimensional reduction performed is valid. Another way would be to check directly if the underlying assumptions of the dimensional reduction holds. This would mean checking the masses of the modes of the relevant fields and comparing these to the matching scale and from this determine if it is possible to perform the dimensional reduction.

References

[1]M. Dine and A. Kusenko, "The Origin of the matter - antimatter asymmetry", Rev. Mod. Phys. **76**, 1 (2003).

[2]D. E. Morrissey and M. J. Ramsey-Musolf, "Electroweak baryogenesis", New J. Phys. **14**, 125003 (2012).

[3]A. Ekstedt and J. Löfgren, "A Critical Look at the Electroweak Phase Transition", JHEP **12**, 136 (2020).

[4]S. Kanemura and Y. Mura, "Electroweak baryogenesis via top-charm mixing", (2023).

[5]T. D. Lee, "A Theory of Spontaneous T Violation", Phys. Rev. D **8**, edited by G. Feinberg, 1226–1239 (1973).

[6]J. O. Andersen, "Dimensional reduction of the two Higgs doublet model at high temperature", Eur. Phys. J. C **11**, 563–570 (1999).

[7]A. Ekstedt, P. Schicho, and T. V. I. Tenkanen, "DRalgo: a package for effective field theory approach for thermal phase transitions", (2022).

[8]P. Basler, M. Krause, M. Muhlleitner, J. Wittbrodt, and A. Wlotzka, "Strong First Order Electroweak Phase Transition in the CP-Conserving 2HDM Revisited", JHEP **02**, 121 (2017).

[9]H. E. Haber and O. Stål, "New LHC benchmarks for the $\mathcal{CP}$ -conserving two-Higgs-doublet model", Eur. Phys. J. C **75**, [Erratum: Eur.Phys.J.C 76, 312 (2016)], 491 (2015).

[10]C. L. Wainwright, "CosmoTransitions: Computing Cosmological Phase Transition Temperatures and Bubble Profiles with Multiple Fields", Comput. Phys. Commun. **183**, 2006–2013 (2012).

[11]J. Oredsson and J. Rathsman, "$\mathbb{Z}_2$ breaking effects in 2-loop RG evolution of 2HDM", JHEP **02**, 152 (2019).

[12]G. C. Branco, P. M. Ferreira, L. Lavoura, M. N. Rebelo, M. Sher, and J. P. Silva, "Theory and phenomenology of two-Higgs-doublet models", Phys. Rept. **516**, 1–102 (2012).

[13]J. Goldstone, A. Salam, and S. Weinberg, "Broken Symmetries", Phys. Rev. **127**, 965–970 (1962).

[14]S. L. Glashow and S. Weinberg, "Natural Conservation Laws for Neutral Currents", Phys. Rev. D **15**, 1958 (1977).

[15]S. Davidson and H. E. Haber, "Basis-independent methods for the two-Higgs-doublet model", Phys. Rev. D **72**, [Erratum: Phys.Rev.D 72, 099902 (2005)], 035004 (2005).

[16]I. F. Ginzburg and I. P. Ivanov, "Tree-level unitarity constraints in the most general 2HDM", Phys. Rev. D **72**, 115010 (2005).

[17]I. P. Ivanov, "Minkowski space structure of the Higgs potential in 2HDM. II. Minima, symmetries, and topology", Phys. Rev. D **77**, 015017 (2008).

[18]D. Croon, O. Gould, P. Schicho, T. V. I. Tenkanen, and G. White, "Theoretical uncertainties for cosmological first-order phase transitions", JHEP **04**, 055 (2021).

[19]R. M. Fonseca, "GroupMath: A Mathematica package for group theory calculations", Comput. Phys. Commun. **267**, 108085 (2021).

[20]M. Bertenstam, *Private communication to obtain permission to use his code.*

A Appendix

The conversion from the Higgs basis couplings to the generic basis couplings comes about as a result of the Higgs basis being a rotation of the generic basis. The specific formulas are (formulas are from [15])

$$m_{11}^2 = Y_1 c_\beta^2 - Y_2 s_\beta^2 + Y_3 s_{2\beta} \tag{38}$$

$$m_{22}^2 = -Y_1 s_\beta^2 + Y_2 c_\beta^2 + Y_3 s_{2\beta} \tag{39}$$

$$m_{12}^2 = -\frac{1}{2}(Y_1 - Y_2) s_{2\beta} + Y_3 c_{2\beta} \tag{40}$$

$$\lambda_1 = Z_1 c_\beta^4 + Z_2 s_\beta^4 + \frac{1}{2} Z_{345} s_{2\beta}^2 - 2 s_{2\beta}[c_\beta^2 Z_6 + s_\beta^2 Z_7] \tag{41}$$

$$\lambda_2 = Z_1 s_\beta^4 + Z_2 c_\beta^4 + \frac{1}{2} Z_{345} s_{2\beta}^2 + 2 s_{2\beta}[s_\beta^2 Z_6 + c_\beta^2 Z_7] \tag{42}$$

$$\lambda_3 = \frac{1}{4} s_{2\beta}^2 [Z_1 + Z_2 - 2Z_{345}] + Z_3 + s_{2\beta} c_{2\beta}(Z_6 - Z_7) \tag{43}$$

$$\lambda_4 = \frac{1}{4} s_{2\beta}^2 [Z_1 + Z_2 - 2Z_{345}] + Z_4 + s_{2\beta} c_{2\beta}(Z_6 - Z_7) \tag{44}$$

$$\lambda_5 = \frac{1}{4} s_{2\beta}^2 [Z_1 + Z_2 - 2Z_{345}] + Z_5 + s_{2\beta} c_{2\beta}(Z_6 - Z_7) \tag{45}$$

Where $Z_{345} = Z_3 + Z_4 + Z_5$ is used as a simplifying piece of notation.